Dynamics of Nucleotides in VDAC Channels: Structure-Specific Noise Generation

Tatiana K. Rostovtseva,* Alexander Komarov,†‡ Sergey M. Bezrukov,†‡ and Marco Colombini*

*Department of Biology, University of Maryland, College Park, Maryland 20742, †Laboratory of Physical and Structural Biology, National Institute of Child Health and Human Development, National Institutes of Health, Bethesda, Maryland 20892 USA, and ‡St. Petersburg Nuclear Physics Institute, Gatchina 188350, Russia

ABSTRACT Nucleotide penetration into the voltage-dependent mitochondrial ion channel (VDAC) reduces single-channel conductance and generates excess current noise through a fully open channel. VDAC channels were reconstituted into planar phospholipid membranes bathed in 1.0 M NaCl. At a given nucleotide concentration, the average decrease in small-ion channel conductance induced by mononucleotides ATP, ADP, AMP, and UTP and dinucleotides β- and α-NADH, NAD, and NADPH are very close. However, the excess current noise is about seven times higher in the presence of NADPH than in the presence of ATP and is about 40 times higher than in the presence of UTP. The nucleotide-generated low-frequency noise obeys the following sequence: β-NADPH $>$ β-NADH $=$ α-NADH $>$ ATP $>$ ADP $>$ β-NAD $\geq$ AMP $>$ UTP. Measurements of bulk-phase diffusion coefficients and of the effective charge of the nucleotides in 1.0 M NaCl suggest that differences in size and charge cannot be the major factors responsible for the ability to generate current noise. Thus, although the ability of nucleotides to partition into the channel's pore, as assessed by the reduction in conductance, is very similar, the ability to generate current noise involves a detailed recognition of the three-dimensional structure of the nucleotide by the VDAC channel. A possible mechanism for this selectivity is two noise-generating processes operating in parallel.

INTRODUCTION

Some of the dynamics of membrane channels are encoded into the time-dependent changes in the current flowing through channel pores. This encoding, referred to as current noise, contains information on changes in the structure and charge distribution of the channel former and its immediate environment. The analysis of current noise has been used to gain information on the channel gating kinetics (Conti and Wanke, 1975; Neher and Stevens, 1977; DeFelice, 1981, Van Driessche, 1994), pore residue protonation (Prod'hom et al., 1987; Pietrobon et al., 1988; Bezrukov and Kasianowicz, 1993; Kasianowicz and Bezrukov, 1995; Rostovtseva et al., 2000), and detailed motions in the permeation path (Sigworth, 1985; Heinemann and Sigworth, 1990). It has also been used to probe the nature and interaction with the channel of permeating molecules such as neutral polymers (Bezrukov et al., 1994, 1996; Bezrukov, 2000), short pieces of DNA (Kasianowicz et al., 1996; Akeson et al., 1999; Henrickson et al., 2000; Meller et al., 2000) and metabolite molecules (Nekolla et al., 1994; Andersen et al., 1995, 1999; Rostovtseva and Bezrukov, 1998; Bezrukov et al., 2000b; Hilty and Winterhalter, 2001). The insights gained from the information collected have been limited by a variety of technical difficulties but also, to a significant degree, by our very limited understanding of the dynamics and electrostatics of these narrow aqueous pathways through complex macromolecules. The reason for this is that the information obtained from the current noise must be applied to a preconceived model of the source of the noise, and, if the model is deficient or wrong, so is the interpretation. Though this statement is quite general and applies to any physical model including, for example, models for reversal potentials, the dynamics of aqueous pores through channels present special challenges.

Large membrane channels allow the passage of both higher molecular-weight molecules and small current-carrying ions that can interfere with each other resulting in current noise. This noise contains information on their interaction, which gives insight into the permeation process. Nonelectrolyte polymers interfere with the flux of small ions decreasing channel conductance (Krasilnikov et al., 1992; Merzlyak et al., 1999) and causing noise (Bezrukov and Vodyanoy, 1993; Bezrukov et al., 1994, 1996; Parsegian et al., 1995; Bezrukov and Kasianowicz, 1997, 2001). This has been used to estimate the diffusion coefficient within the aqueous pore, to measure the diameter of the pore, and even to make inferences on the shape of the walls of the pore (Rostovtseva et al., 2001). This mode of noise generation has been called the molecular "Coulter counter" process because it functions, at the microscopic level, similarly to the macroscopic device of the same name that is used to count cells as they pass through a small orifice (Bezrukov, 2000). The same principle applies to macromolecule transport through nuclear pore complexes (Bustamante et al., 1995).

The large channel examined in this report is a highly conserved monomeric protein located in the mitochondrial outer membrane, called voltage-dependent mitochondrial ion channel (VDAC). This 30-kDa β barrel forms an aque-

Received for publication 16 July 2001 and in final form 16 September 2001.

Address reprint requests to Marco Colombini, Univ. of Maryland, Lab. Of Cell Biology, Dept. of Zoology, College Park, MD 20742-4415. Tel.: 301-405-6925; Fax: 301-314-9358; E-mail: mc34@umail.umd.edu.

0006-3495/02/01/193/13 $2.00

ous pore 2.5 to 3 nm in diameter (Mannella et al., 1989; Blachly-Dyson et al., 1990; Song et al., 1998) that allows the passage of ATP and other metabolites through the outer membrane. Gating of VDAC has been shown to be capable of controlling the flow of metabolites (Hodge and Colombini, 1997; Rostovtseva and Colombini, 1996, 1997). Closure of VDAC and the subsequent failure to exchange metabolites between the cytosol and mitochondria has been linked to the initiation of apoptosis (Vander Heiden et al., 2000, 2001).

To investigate the mechanism of ATP permeation through the open VDAC channel, Rostovtseva and Bezrukov (1998) examined the ability of ATP to interfere with the current carried by small ions through single channels reconstituted into planar membranes. They showed that ATP permeation reduced the VDAC channel conductance and increased the current noise through the fully open channel. They concluded that ATP concentrates within the confines of the VDAC pore perhaps due to the presence of a binding site. In the work presented here, we sought to determine whether the conductance changes and noise generation observed with ATP were a manifestation of the Coulter counter process or arose from a mechanism with higher specificity. We chose molecules similar to ATP, other nucleotides of physiological interest, but differing in size, charge, and core structure. Our results show that, although the ability of individual nucleotides to reduce single-channel conductance is rather nonspecific, the ability to generate noise depends on their detailed three-dimensional structure. The latter is proposed to arise from a specific binding mechanism.

MATERIALS AND METHODS

Chemicals

The following nucleotides were purchased from Sigma Chemical Co. (St. Louis, MO): ATP, β-NADH and α-NADH as disodium salts; UTP and β-NADPH as tri- and tetrasodium salt; ADP, AMP as a monosodium salt; and β-NAD. Three sugars with known diffusion coefficients in water were used: glucose (Sigma), sucrose (Bio-Rad laboratories, Richmond, CA) and raffinose (Aldrich Chemical Company, Inc., Milwaukee, WI). If not specified, the NAD, NADH, and NADPH used in the experiments was the naturally occurring, β, form.

Noise and single-channel conductance measurements

VDAC channels were isolated from *Neurospora crassa* mitochondrial outer membranes and purified according to standard methods (Mannella, 1982; Freitag et al., 1983). Bilayer membranes were formed from monolayers made from a 1% solution of diphytanoylphosphatidylcholine (Avanti Polar Lipids, Inc., Alabaster, AL) in hexane (Aldrich Chemical Company, Inc.) on a 70–90-μm-diameter aperture in a 15-μm thick Teflon partition that separated two chambers (modified Montal and Mueller [1972] technique). The total capacitance was 70–80 pF and the film capacitance was 30–35 pF. Aqueous solutions of 1.0 M NaCl and 1 mM $CaCl_2$ were buffered by 5 mM HEPES at pH 8.0–8.2. All measurements were made at room temperature (23.0 $\pm$ 1.5)°C.

Single-channel insertion was achieved by adding 0.1–0.3 μl of a 1% Triton X100 solution of purified VDAC to the 2.0 ml aqueous phase in the "*cis*" compartment while stirring. After a single channel was inserted and its parameters were recorded, membrane-bathing solutions in both compartments were replaced by nucleotide-contained solutions. In this way, the effects of nucleotides were observed on the same channel. At the end of each experiment, the contents of both compartments were taken to measure conductivity using a CDM 80 conductivity meter (Radiometer, Copenhagen, Denmark) to verify the effectiveness of the perfusion. The concentrations of NADPH, NADH, and NAD in both compartments were measured by absorbance at 259 and 340 nm. Therefore, the nucleotides concentrations shown in the graphs correspond to the actual nucleotide concentrations in the experimental chamber.

Addition of nucleotides to 1.0 M NaCl solutions followed by neutralization to pH 8.0 resulted in dilution of the sodium chloride. Thus, conductance measurements made of the bulk solution and on channels were compared to the control sodium chloride solution diluted to the same extent with water. Only relative conductances are reported because we are interested in how the nucleotides change the conductance of the medium.

The membrane potential was maintained using Ag/AgCl electrodes with 3.0 M KCl, 15% agarose bridges assembled within standard 200-μl pipette tips (Bezrukov and Vodyanoy, 1993). Potential is defined as positive when it is greater at the side of protein addition (*cis*). The current was amplified by a Dagan 3900 integrating patch-clamp amplifier (Dagan Corp., Minneapolis, MN) with a 3902 headstage or by an Axopatch 200B amplifier (Axon Instruments, Inc., Foster City, CA) in the voltage clamp mode. Data were filtered by a low-pass eight-pole Butterworth filter (Frequency Devices, Haverhill, MA) at 15 kHz and recorded simultaneously by a VCR operated in a digital mode and a chart recorder, and directly saved into the computer memory with a sampling frequency of 50 kHz. Amplitude analysis was done using software developed in-house. The membrane chamber and headstage were isolated from external noise sources with double high-μ metal screen (Amuneal Manufacturing Corp., Philadelphia, PA).

Because, for equilibrium sources of conductance fluctuations, the amplitude of the current noise power spectrum is proportional to the square of the current (DeFelice, 1981; Kasianowicz and Bezrukov, 1995) it was necessary to compensate for differences in dilution of sodium chloride resulting from neutralization of the added nucleotide. All values were adjusted to a final concentration of 1.0 M NaCl.

Measurements of the bulk diffusion coefficients

We assumed that the diffusion rates of ATP, β-NADH, and sucrose molecules through a 0.45-μm millipore filter were essentially the same as in the bulk solution, due to the relatively small Stokes radius of these molecules compared to the dimensions of the filter pores. The millipore filter (Millipore Filter Corporation, Bedford, MA) was clamped across the 0.6-cm hole between two 2.2-ml compartments of the experimental chamber. Aqueous solutions were degassed under vacuum before experiments to prevent any blockage of the filter by air bubbles. The filter was surrounded by symmetrical solutions of 1.0 M NaCl buffered with 5 mM HEPES at pH 8.0. To equilibrate the hydrostatic pressure between the two compartments, they were connected using an 8-cm-long U-tube for 15 min. The U-tube was clamped (isolating the chambers) before addition of the sample containing the test solute. This sample, 200 μl of 1.0 M NaCl solution containing sucrose and either ATP or NADH, buffered by 5 mM HEPES at pH 8.0, was added to the *cis* compartment to a final concentrations of 13.6 mM sucrose with 4.1 mM ATP or 6.0 mM NADH. The same volume of 1 M NaCl buffer solution was added simultaneously into the *trans* side. The solutions in both compartments were stirred continuously, and 50-μl samples were taken every 5 min from the *trans* compartment. The volume

on the *trans* side was maintained by the addition of the same amount of fresh stock solution.

The sucrose content in the 50-μl samples was determined by the method described in Dische (1953) by measuring the absorbance at 635 nm. The concentrations of ATP or NADH in the samples were checked spectrophotometically. All assays were calibrated using the pure chemicals or published extinction coefficients.

Calculation of diffusion coefficient

The flux of the solute across the membrane filter obeyed first-order kinetics. Because significant amounts of solute often accumulated on the *trans* side, resulting in significant back-flux, the following integrated form of the rate equation was used:

$$kt = \frac{1}{2}\ln\left(\frac{1}{1 - 2(c/c_{cis})}\right), \quad (1)$$

Where k is the rate constant, c_{cis} is the initial solute concentration in *cis* compartment, and c is the concentration in the *trans* compartment at any time, t. The diffusion coefficient, D, is related to k by equating Fick's law to the rate equation,

$$\text{Flux} = DS\frac{\Delta c}{\Delta x} = k\Delta cv, \quad (2)$$

where S is the area of the membrane, Δc is the concentration gradient, Δx is the effective thickness of the filter, and v is the volume on the *trans* side. The known diffusion coefficient for sucrose (Weast, 1979), $D_{sucr} = 0.521 \times 10^{-5}$ cm^2/s, was used to determine the ratio $S/\Delta x$ allowing D for ATP and NADH to be calculated from k. To further reduce experimental variability, the fluxes of ATP or NADH were measured simultaneously with sucrose. Values are reported as means ± SD.

Estimation of net charge on the nucleotides

According to our titration curves performed in the presence of 1.0 M NaCl and 50 mM nucleotide, the phosphate groups were fully deprotonated by pH 8.0. However, at high sodium concentrations, significant sodium binding is expected. To estimate the total free charge carried by these molecules, the amount of free Na^+ was measured with a sodium electrode (Model 86–11, Orion Research Inc., Beverly, MA) in solutions of 100 mM nucleotides also containing 1.0 M NaCl at pH 8.0. Freshly prepared nucleotide solutions were used. The electrode was equilibrated with each sample (5 ml) for 10 min under continuous stirring. The calibration curve was measured at the same time. The amount of Na^+ bound was determined by subtracting the free [Na^+] (measured by Na^+ electrode) from the total [Na^+]. The latter included the Na^+ from the NaOH used to neutralize the sample and any Na^+ present in the reagent as purchased, assessed using a flame spectrophotometer (Model 560 Perkin-Elmer, Norwalk, CT) reading the absorbance at 589 nm.

The Na^+ electrode was calibrated against NaCl solutions, and so these measurements assume the same value for the activity coefficient. Because there is almost no change in the activity coefficient between 1.0 and 1.5 M NaCl, the assumption seems to be valid. Subtracting the bound Na^+ per mole from the expected charge of the nucleotide in dilute solutions yields the effective free charge on the solute.

Fluorescence measurements

We noticed an increase in the intensity of color of the NADH solution upon addition of NAD, which itself forms colorless solutions. We were concerned that complexes may be formed between these molecules and that these could account for the ability of NAD to interfere with noise formation by NADH by a mechanism that does not involve competition for a binding site. We checked for possible complex formation by fluorescence. Mixtures of NADH and NAD (4:7) yielded the same emission spectra, 410–600 nm, when two different excitation wavelengths, 340 and 400 nm, were used. (The NADH concentration was varied from 10 to 40 mM.) This indicated the presence of a single fluorophore. Thus, no evidence was found for significant complex formation. The obvious color change is attributed to the exchange of electrons between NAD and NADH in the concentrated solutions, resulting in novel extended absorption bands.

RESULTS

The experiments focused on the highest conducting state of the VDAC channel, the open state. All measurements were restricted to this state and thus were made on single or, rarely, two channels to be certain that data collected referred to the open state. This is the state that is permeable to nucleotides (Rostovtseva and Colombini, 1996) and the aim was to gain insights into nucleotide permeation by observing how the permeation process interfered with the movement of small ions. Thus, current noise arising from any gating process was carefully avoided.

Previous observations had shown (Rostovtseva and Bezrukov, 1998) that ATP permeation reduced the flow of small ions, resulting in a reduction in conductance and an increase in current noise. The reduction in conductance was interpreted as the entry of ATP, reducing the number of small ions in the channel lumen. The entry and exit of ATP would then result in fluctuations in the current carried by small ions. This interpretation, based on simple obstruction of the flow of current-carrying ions, makes straight-forward predictions, such as dependence of current noise on the size of the nucleotide. The results we present here indicate a more complex mechanism.

Nucleotides generate current noise in VDAC channels

The noise measured arose primarily from fluctuations in the current carried by small ions (Na^+ and Cl^-). Because noise level depends on the square of the ion current and because the noise through the open state is small, reliable measurements required the use of high levels of salt, so 1.0 M NaCl was chosen.

The addition of nucleotides causes two effects: a decrease in the mean current through a VDAC channel (Fig. 1 *A*) and an increase in its current noise (Fig. 1 *B*). The left trace is a control record of a fully open channel at +50 mV applied potential. The right trace shows the drop in a mean current through the same fully open channel after the 1.0 M NaCl bathing solutions on both sides of the membrane were replaced by 1.0 M NaCl solutions containing 74 mM NADPH. To avoid the limitations imposed by conductance variation among single VDAC channels, current recordings with and without nucleotides were made on the same channel.

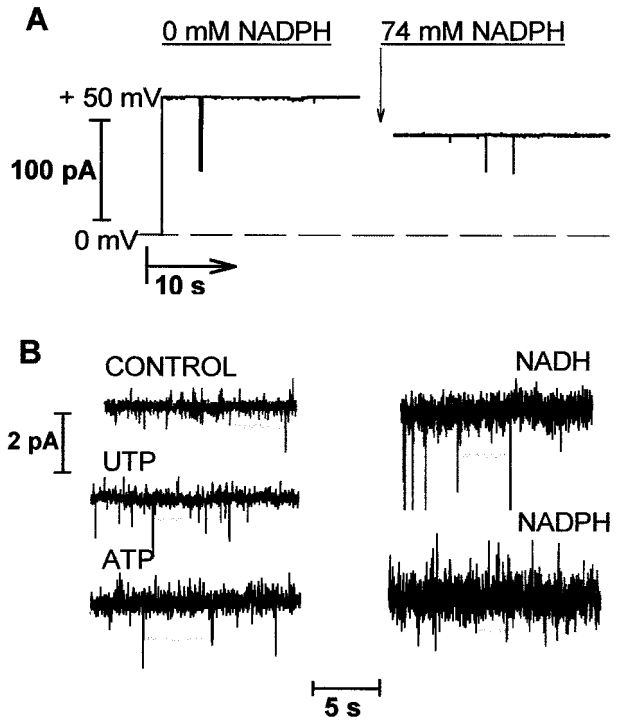

FIGURE 1 Ionic currents through a single VDAC channel are altered by the addition of nucleotides. (*A*) Addition of NADPH decreased the mean current. The recordings were made on the same single channel *(left to right)* without nucleotide by using 0 mV and +50 mV applied potential, and, after addition of 74 mM NADPH, at +50 mV applied potential. The dashed line shows the zero-current level. (*B*) The current traces show the recording at a finer scale without nucleotide addition (*control*) and after addition of 74 mM UTP, 76 mM ATP, 67 mM NADH, and 74 mM NADPH at +50 mV applied potential. Note that excess current noise depends on the type of nucleotide present in solution. The short horizontal bars show examples of the fragments selected for current noise analysis. The solutions contained 1.0 M NaCl and 5 mM HEPES at pH 8.0. Current records were filtered using averaging time of 9 ms. The sign of the potential refers to the side of the membrane to which nucleotide was added.

Figure 1 *B* shows the currents through fully open VDAC channel at a finer scale in the presence of different mono- and dinucleotides. There are large differences in current noise depending on which nucleotide is present. The greatest current noise was induced by NADPH. Intermediate levels were observed with NADH and ATP. UTP barely produces any detectable increase above the control. Note that the ability to generate noise seems almost unrelated to size and charge of nucleotide (see Table 1). This unexpected result indicates a noise-generating mechanism that is more complex than simple obstruction.

In selecting the current fragments suitable for noise analysis, large amplitude events, presumably corresponding to motion of the protein (e.g., gating), were excluded. The short horizontal bars in Fig. 1 *B* show the fragments selected for analysis. Thus, differences in noise level cannot be attributed to effects of nucleotides on the gating of VDAC.

TABLE 1 Bulk properties of different nucleotides are very similar

Nucleotide	Amount of Bound Na^+	Molecular Weight with Bound Na^+	Free Negative Charge	Diffusion Coefficient ($\times 10^{-6}$ cm^2/s)
ATP^{-4}	2.6	563	−1.4	4.5 ± 0.3
ADP^{-3}	1.6	461	−1.4	—
AMP^{-2}	1.0	370	−1.0	—
UTP^{-4}	2.5	538	−1.5	—
$NADPH^{-4}$	2.0	786	−2.0	—
$NADH^{-2}$	0.9	685	−1.1	3.3 ± 0.2
NAD^{-1}	1.0	686	0	—

Measurements of current noise amplitude depend on frequency band chosen so quantitation must take into consideration the frequency dependence. Figure 2 illustrates examples of current spectral densities for single VDAC channels in the presence of 74 mM NADPH and 93 mM NAD (*top two traces*, *solid lines*) in comparison with control (*dotted line*) at +50 mV applied potential and the background noise at 0 mV (*bottom trace*). The relatively high conductance of a single VDAC channel (3.4 nS) contributed significantly to the level of the background noise as compared to that of the unmodified membrane (*dashed arrow*). Our investigation of the processes responsible for noise generation is limited to the additional noise induced by the added nucleotide.

The observed noise is "white," i.e., the amplitude of its spectral components is independent of frequency. (The rise in noise level above 1000 Hz seen for NAD, control, and background traces, arises from the instrumentation (Sherman-Gold, 1993). Likewise, the slight decrease in the noise spectrum for NADPH at high frequencies is related to amplifier filtering.)

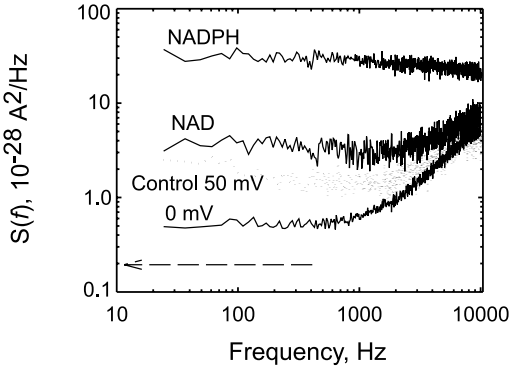

FIGURE 2 The power spectral density of current noise of a single open VDAC channel (*dotted line, control*) in comparison with noise in the presence of 74 mM NADPH (*upper trace*) and 93 mM NAD (*solid line in the middle)* at +50 mV applied voltage. The background noise was obtained at 0 mV (*lower trace*). The level of white noise induced by NADPH is higher than that induced by NAD, which is slightly above the channel noise without nucleotide addition. The increase in spectral density at high frequencies comes from the recording system. The horizontal arrow corresponds to the noise level of the unmodified membrane.

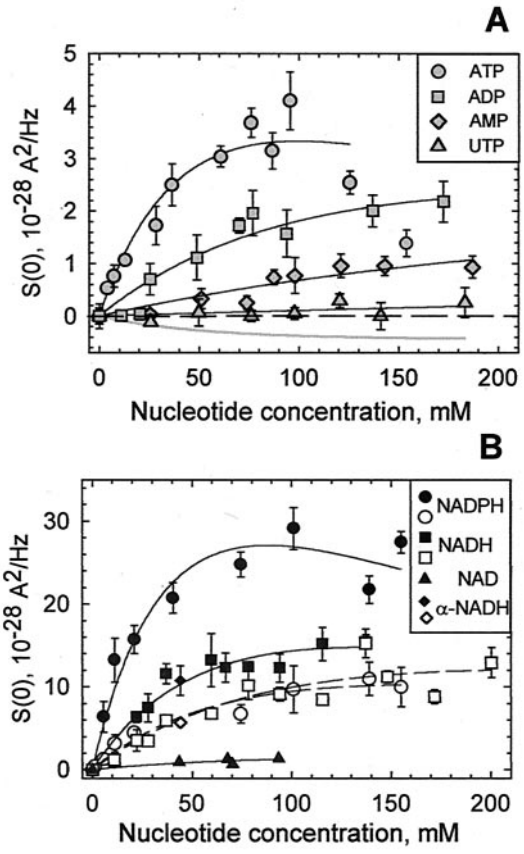

FIGURE 3 The excess current noise recorded through single VDAC channels depends on the type of nucleotide added and its concentration. The low-frequency spectral density, $S(0)$, was plotted as a function of (*A*) mono- and (*B*) dinucleotide concentrations with $S(0)$ without nucleotide addition subtracted. Each point represents an average over the frequency range $100 < f < 1{,}000$ Hz at +50 mV (*filled symbols*) and −50 mV (*open symbols*) with the background subtracted (that is, spectral density of channel noise at 0 mV). Gray line (*A*) shows the estimated reduction of the current noise of the control level due to the reduction of the conductance in the presence of UTP. The theoretical curves were fitted to the data using Eq. 7 with two adjustable parameters. If we assume that the background noise is proportional to the current squared, then the reduction in current induced by UTP would have reduced the control level as shown by the solid gray line.

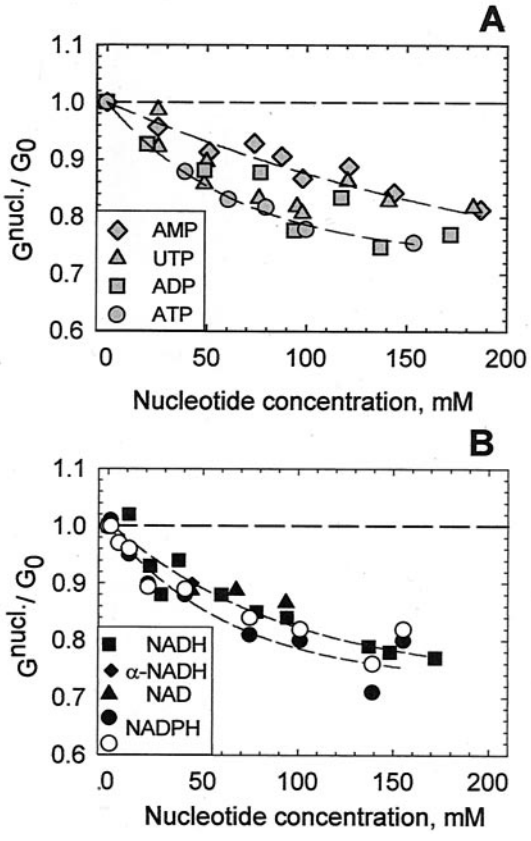

FIGURE 4 The effect of nucleotide addition on VDAC channel conductance in the presence of (*A*) mono- and (*B*) dinucleotides. Conductances are expressed as ratios to corresponding values in nucleotide-free solutions. The unchanged conductance is represented by the horizontal dashed line. The solid lines were obtained from fits to $\Delta G/G_0 = a\{1 - \exp(-b[\text{Nucl.}])\}$, where ΔG is the nucleotide-induced channel conductance reduction, G_0 is channel conductance without nucleotide addition, [Nucl.] is nucleotide concentration in mM, and a and b are fitting parameters adjusted for each nucleotide.

This indicates that the processes generating the noise are very fast (faster that 10 kHz), and so we are likely measuring the noise level in the plateau region of a Lorentzian. This was true for all nucleotides tested. The frequency-independent character of the noise allows us to characterize it by averaging the low frequency portion of the spectral density between 100 and 1000 Hz.

The low-frequency spectral density, $S(0)$, plotted in Fig. 3 was obtained by subtracting this average before and after nucleotide addition for the same channel. ATP, ADP, and AMP all increase open-channel noise but to different extents (Fig. 3 *A*). Note that the level of noise is given in a log scale and so the changes are substantial. The ability to induce noise follows the sequence: ATP > ADP > AMP, indicating a correlation with size and charge, but then, UTP, the same size and charge as ATP, generates virtually no noise. The theory that this might be due to inability of UTP to enter the channel is not correct, because addition of UTP decreases the average current through the channel to about the same extent as does ATP (Fig. 4 *A*). Therefore UTP still contributes to the open-channel noise, but only to the extent that compensates the expected decrease in the channel noise (below the control level shown by the solid gray line) resulting from the conductance decrease. With this correction, the noise generation by UTP is highly statistically significant (at the 95% or 99.5% level in a two-tailed *t*-test, depending on the [UTP]).

Because the only difference between ATP and UTP is that ATP has a purine base and UTP has a pyrimidine base, this base must account for the observed 6–7-fold reduction in noise. GTP generated a level of current noise similar to ATP (data not shown for figure clarity). Such specificity in noise generation cannot be explained by a simple obstruction model such as the Coulter counter process.

Adenine-containing dinucleotides generate current noise

If the presence of a purine base is key to noise generation, then dinucleotides containing a purine base should also generate noise. In addition, the study of dinucleotides could further assess any relationship between molecular size and noise generation. The addition of β-NADPH and β-NADH dramatically increases the open-channel noise (Fig. 3 *B*, *filled symbols*). In comparison to the ATP-induced current noise, the low-frequency spectral density is about seven times higher in the presence of NADPH (still the β form unless otherwise indicated) and four times higher in the presence of NADH. By contrast, β-NAD addition produced a level of current noise only slightly above the control. Perhaps a certain amount of charge is also a requirement for noise generation, because, compared to NADH, NAD as one less negative charge and NADPH as two more negative charges. This sequence, $NADPH^{-4} > NADH^{-2} > NAD^{-1}$, is consistent with the sequence of noise generation observed with adenine mononucleotides, $ATP^{-4} > ADP^{-3} > AMP^{-2}$.

The level of nucleotide-induced noise depends on the sign of the applied potential. Positive potentials (Fig. 3 *B*, *filled symbols*) generate a larger noise signal in the presence of both NADH and NADPH. (In a few experiments, the opposite polarity was observed, and we conclude that, in those, the channel was oriented in the opposite direction.) Because all conditions except for VDAC addition were symmetrical, the asymmetry must arise from the inherent asymmetry of VDAC (Colombini, 1994; Colombini et al., 1996). The ATP-induced current noise was also smaller at negative than at positive potentials (data not shown for the sake of illustration clarity). Note that, at negative applied potentials, the noise is the same for NADH and NADPH (Fig. 3 *B*, *open symbols*), whereas, at positive potentials, the NADPH-induced current noise is two times higher as compared to NADH. To test whether the noise-generation process was specific for the physiological form of NADH (i.e., the β form), we tested the nonphysiological isomer, α-NADH (the nicotinamide moiety is reoriented by 180°). The same level of noise was observed with α-NADH (Fig. 3 *B*, *diamond*) as with β-NADH.

The ability of nucleotides to generate excess noise is uncorrelated with their ability to reduce single-channel conductance

The ability of nucleotides to induce the excess current noise must reflect the ability of these nucleotides to alter current flow through the channels. This could occur if the larger anions interfere with the flow of the smaller ions and reduce channel conductance. The relative changes in the single-channel conductance as a function of mono- and dinucleotides concentration are shown in Fig. 4, *A* and *B*. All nucleotides, whether they generate excess current noise or not, reduce the VDAC channel conductance in 1.0 M NaCl to a similar extent. Note that the concentration dependences of this reduction are also very close for all the nucleotides. Furthermore, the drop of the channel conductance does not depend on the sign of the applied potential (Fig. 4 *B*). Thus, noise generation and reduction in conductance appear to be uncorrelated in contrast to expectations from an obstruction model of noise generation.

The observed decrease in channel conductance could arise from changes in bulk-phase conductivity due to the added nucleotide or the Coulter-counter process. The difference in bulk conductivities might underlie the different observed levels of noise generation. Changes in bulk conductivity due to nucleotide addition include a negative effect of nucleotide interfering with small ion's conductivity and a positive contribution from the conductivity of the charged nucleotide molecules itself plus any counterions (Rostovtseva and Bezrukov, 1998). In our solution preparation procedure (see Methods), these two effects nearly cancel out in the case of ATP and other mononucleotides (data not shown). Addition of dinucleotides reduce bulk solution conductivity, so that the negative effect of dinucleotides dominates in 1.0 M NaCl solutions. However, the decrease in channel conductance is much more pronounced than is the reduction in bulk solution conductivity. Thus the reduction in channel conductance over and above effects on bulk conductivity indicate that the nucleotides penetrate into the channel lumen. This penetration causes noise whose level cannot be accounted for by channel conductance drops, even after compensating for different levels of bulk-phase conductivity.

Ability to generate noise is uncorrelated to the bulk properties of the nucleotides

To determine whether differences in noise generation might arise from differences in the effective size or charge of the solutes, we measured the diffusion coefficient of the nucleotides and the net charge in the same salt solution used in the experiments with VDAC channels. The diffusion coefficients (Table 1) of ATP and β-NADH (averages of three experiments) show that the effective sizes of ATP and NADH are very close, and thus, differences in size are unlikely to account for differences in the ability to generate noise.

Although the pK values of these molecules are known at the high salt concentration used, some Na^+ could bind, reducing the net charge. The amount of Na^+ bound was determined by measuring the total Na^+ and the free $[Na^+]$. ATP and UTP have essentially the same net charge (Table 1), and, therefore, a difference in charge cannot account for the observed differences in ability to generate current noise. The difference in negative charge is more pronounced for dinucleotides, and this might contribute to the larger difference in their ability to generate current noise (Fig. 3).

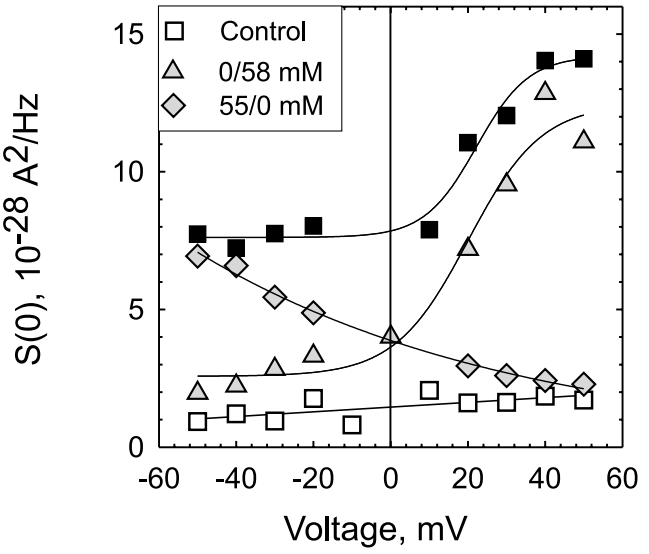

FIGURE 5 The low-frequency current spectral density with asymmetrical NADH addition depends on applied voltage. NADH concentrations on the graph corresponded to NADH additions to the aqueous solution (1.0 M NaCl and 5 mM HEPES, pH 8.0) on either the *cis* or *trans* side of the membrane. Spectral density, $S(0)$, was recalculated for that expected for 50 mV applied voltage (square dependence of noise on applied voltage).

Evidence for a nucleotide binding site within the channel lumen

The apparent ability of the channel to distinguish between purine- and pyrimidine-containing nucleotides (with regard to noise generation) indicates the presence of a binding site. There is also published evidence for an ATP binding site (Flörke et al., 1994, Rostovtseva and Colombini, 1997). However, the mechanism of open-channel noise generation that we propose requires a binding site within the pore of the channel close to the ion stream. To distinguish between a site inside the channel as opposed to a site located on one or the other surface of the protein, we examined the ability of β-NADH to generate current noise when added only to one side of the membrane. After recording the properties of the channel, NADH was added only to one side and current records were taken as a function of voltage. Then, the same amount of NADH was added to the opposite side to obtain current records with a symmetrical NADH concentration on the same channel. Figure 5 shows the dependence of the current noise on the applied voltage in the presence of symmetrical and asymmetrical NADH.

Because the intensity of the excess current noise produced by equilibrium conductance fluctuations (i.e., the low-frequency noise, assumed to be generated by conductance fluctuations unperturbed by the applied electric field) is expected to increase as the square of the applied voltage (e.g., DeFelice, 1981; Fig. 10 *B* in Kasianowicz and Bezrukov, 1995; Fig. 5 in Rostovtseva and Bezrukov, 1998), we recalculated the spectral density, $S_I(0)$, measured at different voltages, to 50 mV. After this correction, current noise in the presence of NADH shows a significant change with voltage in both symmetric and asymmetric experiments. Therefore, in this case, the nucleotide-induced noise is not proportional to the applied voltage squared. Addition of NADH to only one side of the membrane resulted in less noise, indicating that the putative binding site was not present on either surface of the VDAC channel but perhaps within the pore. When NADH was present only in *trans* side (Fig. 5, *gray triangles*) the current noise increased when a positive potential (positive on *cis* side) was applied. This positive potential should drive NADH into the channel and the observed increase in noise with increasing voltage is consistent with the voltage, increasing the NADH concentration inside the channel. When the potential reached +50 mV, the amplitude of the noise approached a value close to that observed with NADH on both sides. When negative potentials were applied, the opposite occurred. The current noise decreased, consistent with negative potentials driving NADH out of the channel, and, at high voltages, approached the level observed without NADH. In experiments where NADH was added only to the *cis* side (*gray diamonds*), the effect of the applied potential on the current noise was the opposite. These results are consistent with noise generation being dependent on concentration of nucleotide in the channel near a binding site for the nucleotide.

If indeed the level of current noise depends on the ability of the nucleotide molecule to bind to a site inside the channel, we would expect competition for this binding site among nucleotides with different abilities to generate noise. To test this hypothesis, we examined mixtures of NADH and either NAD or ATP and measured their ability to generate current noise and reduce the single-channel conductance. The results of these competition experiments obtained at positive applied potentials are presented in Fig. 6.

When concentrations of the competitor used were higher than those of NADH (1:2.3 of NADH to either NAD or ATP) significant drops in the noise level (second bars in each set in Fig. 6) were observed as compared to that expected if each nucleotide acted on the channel independently (as might be expected were noise generation the result of obstruction by nucleotides in the channel). The sum of the noise generated by each nucleotide (when tested separately) is shown in the first bar from the left in each set. The third bars show the results of a theoretical calculation (see Discussion). No significant drop in NADH-induced noise was observed at negative potentials with either ATP or NAD as a competitor, and this may be due to the lower level of noise at negative potentials. In contrast to the nonadditive effect of the noise generated when two nucleotides were mixed, the channel conductance decreased proportionally to the sum of two nucleotides, indicating no competition in the ability to occupy the channel.

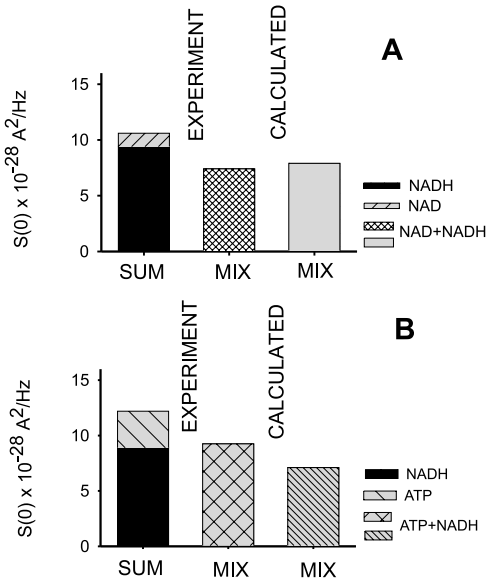

FIGURE 6 The competition experiments. When NADH was mixed with nucleotides with a lower ability to generate the current nose, the noise level was reduced. The mixtures of (*A*) 38 mM NADH with 86 mM NAD and (*B*) 35 mM NADH with 80 mM ATP generate a lower level of current noise (*second bars*) as compared to the sum of the noise produced by these nucleotides individually (*first bars*). The theoretically expected decrease of current noise (*third bars*) was calculated using the equations described in the Appendix with binding constants from Table 2.

Further evidence for a binding site within the lumen of the channel was obtained by measuring changes in reversal potential in the presence of a salt gradient. Nucleotide binding to the site might change the net charge on the wall of the channel, resulting in a change in reversal potential. The reversal potential of a single VDAC channel (in the open state) in the presence of a NaCl salt gradient (500 mM versus 100 mM NaCl) was measured in the absence and presence of 10 mM NADPH on both sides of the membrane. NADPH was chosen because current noise was achieved at fairly low doses, minimizing changes in reversal potential arising merely from the added ions. The reversal potential changed from -20.9 ± 1.7 (4) mV [mean $\pm$ SE (number of experiments)] without NADPH to -13.8 ± 1.2 (4) mV in the presence of 10 mM NADPH. The reduction of 7 mV is consistent with a reduction in the positive charge within the channel of about two negative charges, based on previous work with site-directed mutagenesis (Peng et al., 1992). This result agrees in both sign and magnitude with partial occupancy of a binding within the channel with the negatively charged NADPH.

DISCUSSION

When nucleotides penetrate into VDAC channels, they reduce the single-channel conductance. This reduction is not attributable to a change in the bulk conductance properties of the medium, but the experiments are consistent with a steric effect of larger ions interfering with the flow of smaller ions. This conclusion is supported by saturation at high concentrations and an additive response when two nucleotides are present.

According to the current "diffusion" theory of noise generation (Coulter-counter mechanism), the source of noise is the ability of larger molecules to directly interfere with the small-ion current during their translocation through the channel. The relationship between the low-frequency current density, $S_I(0)$, and particle diffusion coefficient inside the channel, D, is given by (Bezrukov et al., 1994, 2000a)

$$S_I(0) = (\Delta I)^2 \langle N \rangle L^2/3D, \quad (3)$$

where ΔI is the reduction in small-ion current induced by a singe particle entering the channel pore, and $\langle N \rangle$ is the average number of particles in the channel. The particle-diffusion coefficient is inversely proportional to the low-frequency spectral density. If this theory were applied to the current noise generated by the nucleotides, then the mobility of ATP inside the VDAC pore would be about 12 times larger than that of β-NADPH, whereas mobility of UTP would be five times larger than that of ATP (though still smaller than bulk mobility by a factor of 4). The mobility of NADH would be 10 times less than that of NAD.

According to this theory, the same process by which larger molecules interfere with the flow of small ions through the channel causes current noise and reduces the single-channel conductance. However, there is no obvious correlation between the ability of a nucleotide to generate noise and its ability to reduce the single-channel conductance of VDAC. The reduction in single-channel conductance is very similar for all the nucleotides, indicating a similar residency time inside the channel (Fig. 4). This is in stark contrast with their ability to generate current noise because this spans a forty-fold range from barely measurable to highly pronounced.

We propose the presence of two noise-generating processes within the channel. One is a random walk within the channel that slows down ion flow, resulting in a reduced conductance (the Coulter-counter effect). This should produce noise, but, perhaps, in our experiments, the spectral width of this noise is too high and, therefore, the amplitude is too low (Bezrukov et al., 2000a). The low level of noise generated by UTP and NAD may arise from this process. The other process is proposed to involve binding of the nucleotide to a site within the channel. The binding of NADPH, NADH, or ATP to the wall of the channel should increase the negative charge or reduce the positive charge on that surface. This would alter both the conductance and selectivity resulting in a change in current. Thus, binding and unbinding should generate excess current noise. Indeed, it is very difficult to see how the channel could differentiate

between ATP and UTP or between NADH and NAD without using a binding site.

The evidence for a binding site within the channel is quite strong and includes the voltage dependence of noise generation (corrected for the normal square dependence of noise on voltage) when nucleotide was only added to one side, competition among nucleotides with different abilities to generate noise, and changes in reversal potential in the presence of an ion gradient. The large difference in noise generation by ATP and UTP indicates that the binding site shows specificity for a purine base. This was confirmed by experiments with GTP. This apparent specificity extends to the dinucleotides. The nicotinamide portion in the dinucleotides seems not to play an important role in any binding step because changes in orientation of this part of the molecules do not affect noise generation. The same level of noise was observed with β- NADH and its artificial isomer α-NADH.

Charge may also play a factor in the proposed binding process, because noise generation seems to correlate with charge on the nucleotide. It is unclear whether one should consider the net charge on the nucleotide (including Na^+ binding) or the charge excluding Na^+ binding (Table 1). Within the channel, the net charge is positive, and it may be that the binding of the nucleotide excludes the Na^+ ions. The correlation between noise generation and charge on the nucleotide within related groups is present either way, but is more pronounced if Na^+ binding is excluded: $ATP^{-4} > ADP^{-3} > AMP^{-2}$ and $NADPH^{-4} > NADH^{-2} > NAD^{-1}$. This correlation fits very well with the proposed method of noise generation involving binding to the channel wall. It may also explain why NAD has such a small effect despite having a purine base and being the molecule of larger molecular weight than ATP.

Another possibility is that nucleotide binding might increase the motion of the protein, resulting in noise. This would eliminate the need for a change in the charge of the wall of the channel. This motion would not be the slow conformational transitions (such as gating), which we see and do not include in our analysis. Rather, this motion must be fast, perhaps akin to "breathing motions" in proteins (Sigworth, 1985; Nossal and Lecar, 1991). Indeed, without nucleotides present, the open VDAC channel has excess noise. Like conformational changes, motions of the protein do occur, but are far too easy to propose. It seems more parsimonious to propose that the noise arises from electrostatic effects on ion flow rather than protein motion.

The binding-site model of current noise

Binding of charged nucleotides to the wall of the VDAC pore results in a change in the electrostatic profile within the channel. This will likely change the current. Thus, binding and unbinding will cause stochastic unitary changes in current. We can express the binding and unbinding of nucleotide (A) to the VDAC binding site (V), as a first-order kinetic reaction,

$$A + V \underset{\alpha}{\overset{\beta}{\rightleftarrows}} AV, \tag{4}$$

where α and β are the dissociation and association rate constants. This produces fluctuations in current that are described by a two-state Markov process. The phenomenology is identical to the opening and closing of channels, except that these fluctuations happen on top of the average current of a permanently open channel. Thus, we can use the following equation for the spectral density, $S_I(f)$ (Machlup, 1954; DeFelice, 1981; Bezrukov and Kasianowicz, 1993):

$$S_I(f) = 4(\Delta I)^2 \frac{\tau^2}{(\tau_V + \tau_{AV})} \frac{1}{(1 + (2\pi f\tau)^2)}, \tag{5}$$

where ΔI is the difference in current between states V and AV, τ_V and τ_{AV} are the mean times spent in these states, and $\tau = \tau_V\tau_{AV}/(\tau_V + \tau_{AV})$ is the relaxation time in the system. For reaction in Eq. 4,

$$\tau_V = ([A]\beta)^{-1}, \quad \tau_{AV} = \alpha^{-1}, \tag{6}$$

where $[A]$ is nucleotide concentration. At frequencies much lower than the rates of the reaction, $f \ll (2\pi\tau)^{-1}$, the last term in Eq. 5 becomes equal to 1. Thus, the low-frequency limit of the spectral density function, $S_i(0)$, is

$$S_I(0) = \frac{4(\Delta I)^2}{\alpha} \frac{[A]K_{eq}}{(1 + K_{eq}[A])^3}, \tag{7}$$

where the equilibrium constant, $K_{eq} = \beta/\alpha$, is introduced.

The theoretical curves (Fig. 3, *solid lines*) were fitted to the data with two adjustable parameters, K_{eq} and $4(\Delta I)^2/\alpha$. Eq. 7 fits the rising parts of the experimental data rather well. The results of the fitting procedure are presented in Table 2. The expected bell shape of the theoretical fit is clearly seen if the log of the concentration is plotted. From Table 2, it follows that the adenine nucleotides bind to the VDAC pore at positive applied potentials in a sequence: NADPH > ATP > NADH > NAD = ADP > AMP $\gg$ UTP.

TABLE 2 Equilibrium rate constant values obtained from the fitting to binding model

Nucleotide	Sign of the Applied Potential	$4\frac{(\Delta I)^2}{\alpha}$ (A^2 s)	K_{eq} (M^{-1})
NADPH	+V	183	5.7
	−V	69	3.0
NADH	+V	99	3.7
	−V	81	2.2
NAD	+V	10	2.3
ATP	+V	23	5.0
ADP	+V	16	2.0
AMP	+V	11	0.74
UTP	+V	17	0.06

The binding-site model relies on fluctuations in ionic current upon nucleotide binding arising from a change in charge on the wall of the channel due to the binding of the negatively-charged nucleotide. The use of site-directed mutagenesis (Blachly-Dyson et al., 1990) has demonstrated that an increase or decrease in net charge next to the ion stream alters the reversal potential of the VDAC channel in the presence of a salt gradient. From such experiments (see also Peng et al., 1992), we can deduce that the observed decrease in reversal potential by the addition of NADPH is consistent with a decrease in net positive charge on the wall of the channel by ~2 units. This is consistent with the binding of one NADPH molecule of charge −4, because, at 10-mM concentration, the binding site should only be partly occupied. Hence, this observation supports the binding-site model of noise generation.

The binding-site model explains the voltage dependence of noise generation observed in experiments where NADH was added asymmetrically. The occupancy of the binding site depends on the local [NADH], and the applied potential alters the NADH concentration profile within the channel because NADH is negatively charged. Changes in this profile within the channel induced by the electric field can be calculated using the Nernst–Plank flux equations. Figure 7 illustrates the results of these calculations. The calculations assume constant field inside the channel and electroneutrality. They also assume a linear concentration profile inside the channel in the absence of an applied electric field. The channel was taken to be 3.5 nm in length.

If the measured noise depends on the concentration of NADH near the binding site inside the channel (*shaded box*), the voltage-dependence of the noise could be compared to the calculated profiles to determine the location of the binding site. The experimental findings were qualitatively consistent with the calculated profiles. However, the NADH concentration profile would have to be far more sensitive to the applied field than the theoretical calculations would predict. Clearly, the local fields within the channel might strongly influence the profile. The ability of the nucleotide to bind may depend on not only the local concentration of nucleotide but also any field-induced orientation of the free nucleotide that may increase the fraction of successful collisions.

An asymmetrically located binding site could explain the dependence of noise on polarity of the applied potentials. It could be something akin to a rectification process but applied to current noise. The binding-site model can also explain competition among nucleotides for noise generation. Using methods previously described elsewhere (Chen, 1975; Neher and Stevens, 1977), we can calculate the theoretically expected decrease in current noise due to the competition for the binding site between two nucleotides, 1 and 2 (see Appendix).

The third bars in each set in Fig. 6 were calculated using the corresponding binding constants from Table 2. There is good agreement between the theoretically expected values and those experimentally observed (second bars in the set) indicating that the competition can be understood in terms

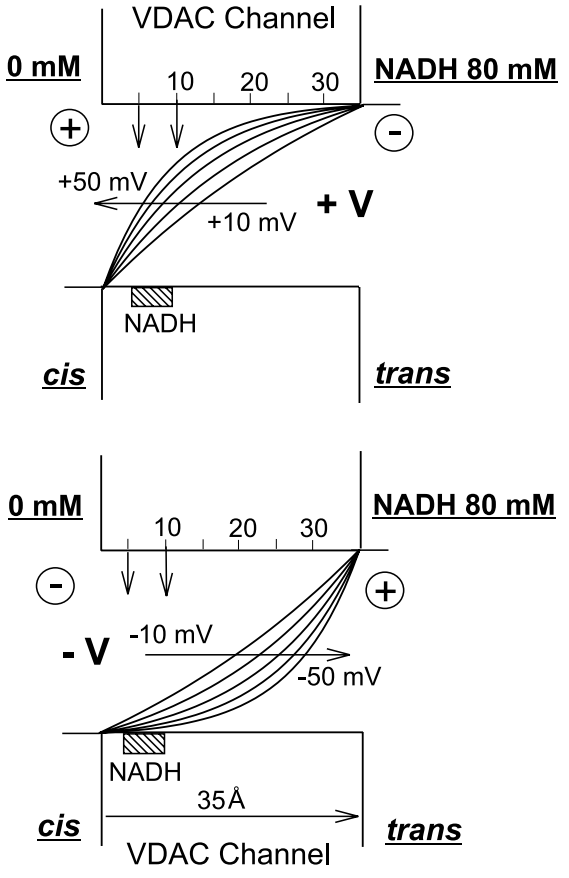

FIGURE 7 The binding site of NADH is located inside the channel lumen. NADH was added asymmetrically forming a concentration gradient inside the channel. The gradient is expected to vary with applied potential. The concentration profiles were calculated using Nernst–Plank flux equations. The channel was assumed to be 3.5 nm long. The measured noise is assumed to depend on the concentration of NADH near the binding side inside the channel (*shaded box*). The voltage drives NADH either into or out of the channel depending on the sign. This accounts for the change in the noise with applied voltage.

of the binding model. In doing the theoretical calculations, we needed the value of the dissociation rate constant, α. Based on the time response of our recording system, we choose a lower limit for α, $10^4\ s^{-1}$. However, we found that the results were very insensitive to the chosen value of α.

The diffusion process and the nucleotide binding are proposed to happen in parallel. The freely diffusing nucleotides are then mostly responsible for the conductance reduction (Fig. 4), but the noise associated with the diffusion process (Eq. 3) is small because diffusion is fast. Nucleotide binding may increase or decrease conductance but not to a significant extent, because it was not detected above the experimental error.

Physiological implications

At first sight, the high nucleotide concentration used in these experiments seems to be hopelessly unphysiological.

Free ATP levels in cells are only a few millimolar. Free NADH and NADPH levels have not been measured accurately, but are likely to be in the tens to hundreds of micromolar. Thus, our measurements are made at concentrations that are two orders of magnitude too high. Are we, therefore, looking at an interesting physical phenomenon that is unrelated to the biology of cells? One way to address this question experimentally is to determine whether our observations are limited to VDAC from the fungus, *N. crassa*, or are conserved in VDAC channels from very diverse species. This research is under way. Another approach is to consider possible physiological roles of the observed selectivity.

VDAC channels are pathways by which metabolites travel between the cytosol and the mitochondrial spaces. Their location in the mitochondrial outer membrane makes them the gatekeepers of metabolite flux between this highly evolutionarily-adapted endosymbiote and its host. At times, the rate of flux through these channels becomes limiting (e.g., times of high energy demand; Gellerich and Kunz, 1987; Gellerich et al., 1993) and this can easily limit survival. Thus, the permeation pathway formed by VDAC may have evolved to accelerate the flow of the most critical metabolites, adenine nucleotides. The presence of binding sites causes a higher effective concentration in the channel and, at low concentrations, will accelerate the flux. At high concentrations, this binding leads to saturation, resulting in reduced flux as compared to a molecule that is not bound. Thus, just as binding to a transporter accelerates substrate flux at low concentrations and slows it down at high concentrations, the same could be true for ATP flux through VDAC. The electrostatic profile that leads to binding at the unphysiologically-high concentrations may favor ATP flux at the low, physiologically-relevant concentrations.

APPENDIX

Conductance noise at competitive binding

Noise of the channel at competitive binding of nucleotide 1 (N1) and nucleotide 2 (N2) can be represented by the following state diagram:

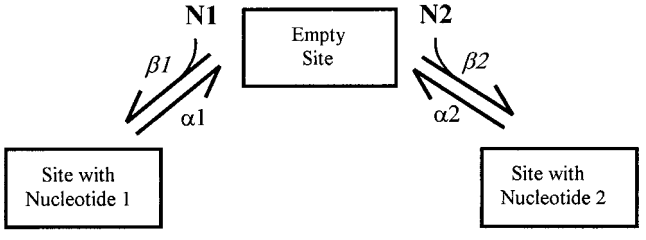

Only the empty site can react with either nucleotide 1 or nucleotide 2. All three states generally differ by their conductance. The current flowing through the channel is changed from the level in the unoccupied state, "empty site", by i_1 when the site accepts nucleotide 1 and by i_2 when it accepts nucleotide 2. For the probabilities of the empty site, $P_0(t)$, the site occupied by nucleotide 1, $P_1(t)$, and the site occupied by nucleotide 2, $P_2(t)$, we have

$$\frac{dP_1(t)}{dt} = -\alpha 1 P_1(t) + \beta 1[N1]P_0(t), \tag{A1}$$

$$\frac{dP_2(t)}{dt} = -\alpha 2 P_2(t) + \beta 2[N2]P_0(t), \tag{A2}$$

$$P_0(t) = 1 - P_1(t) - P_2(t). \tag{A3}$$

Using methods described elsewhere (Chen, 1975; Neher and Stevens, 1977), we arrive at the following expression for the spectral density of current fluctuations:

$$S(f) = (i_1 i_1 \varphi\gamma + i_1 i_2 \varphi\gamma' + i_1 i_2 \varphi'\gamma'^* + i_2 i_2 \varphi'\gamma^*) \frac{4s_1^{-1}}{1 + (2\pi f s_1^{-1})^2} + (i_1 i_1 \varphi\eta + i_1 i_2 \varphi\eta' + i_1 i_2 \varphi'\eta'^* + i_2 i_2 \varphi'\eta^*) \frac{4s_2^{-1}}{1 + (2\pi f s_2^{-1})^2}, \tag{A4}$$

where several abbreviations have been introduced,

$$s_{1,2} = \tfrac{1}{2}[\beta 1[N1] + \alpha 1 + \beta 2[N2] + \alpha 2 \mp \sqrt{(\beta 1[N1] + \alpha 1 - \beta 2[N2] - \alpha 2)^2 + 4\beta 1[N1]\beta 2[N2]}],$$

where s_1 uses the negative square root and s_2 the positive.

$$\varphi = \frac{\beta 1[N1]\alpha 2}{s_1 s_2},$$

equilibrium probability to find the site occupied by nucleotide 1,

$$\gamma = \frac{\beta 1[N1] + \beta 2[N2] + \alpha 2 - s_1 - \varphi s_2}{s_2 - s_1},$$

$$\eta = 1 - \varphi - \gamma;$$

$$\varphi' = \frac{\alpha 1 \beta 2[N2]}{s_1 s_2},$$

equilibrium probability to find the site occupied by nucleotide 2,

$$\gamma' = -\frac{\varphi' s_2}{s_2 - s_1},$$

$$\eta' = -\varphi' - \gamma.$$

Symbols with asterisk (*) are obtained by exchanging indices 1 and 2 for the rate constants, α and β, and nucleotide concentrations.

We thank Alexander Berezhkovskii for discussions. Research for this work was supported by National Science Foundation award # 9816788.

REFERENCES

Akeson, M., D. Branton, J. J. Kasianowicz, E. Brandin, and D. Deamer. 1999. Microsecond time-scale discrimination among polycytidylic acid, polyadenylic acid, and polyuridylic acid as homopolymers or as segments within single RNA molecules. *Biophys. J.* 77:3227–3233.

Andersen, C., M. Jordy, and R. Benz. 1995. Evaluation of the rate constants of sugar-transport through maltoporin (LamB) of *E. coli* from the sugar-induced current noise. *J. Gen. Physiol.* 105:385–401.

Andersen, C., B. Rak, and R. Benz. 1999. The gene bglH present in the bgl operon of *Escherichia coli*, responsible for uptake and fermentation of beta-glucosides encodes for a carbohydrate-specific outer membrane porin. *Mol. Microbiol.* 31:499–510.

Bezrukov, S. M. 2000. Ion channels as molecular Coulter counters to probe metabolite transport. *J. Membr. Biol.* 174:1–13.

Bezrukov, S. M., A. M. Berezhkovskii, M. A. Pustovoit, and A. Szabo. 2000a. Particle number fluctuations in a membrane channel. *J. Chem. Phys.* 113:8206–8211.

Bezrukov, S. M., and J. J. Kasianowicz. 1993. Fluctuations in current through a single open ion channel reveal titration kinetics of ionizable residues. *Phys. Rev. Lett.* 70:2352–2355.

Bezrukov, S. M., and J. J. Kasianowicz. 1997. The charge state of an ion channel controls neutral polymer entry into its pore. *Eur. Biophys. J.* 26:471–476.

Bezrukov, S. M., and J. J. Kasianowicz. 2001. Dynamic partitioning of neutral polymers into a single ion channel. *In* Structure and Dynamics of Confined Polymers. J. J. Kasianowicz, M. S. Kellermayer, and D. W. Deamer, editors. Kluwer Publisher, Dordrecht, The Netherlands. 93–106.

Bezrukov, S. M., L. Kullman, and M. Winterhalter. 2000b. Probing sugar translocation through maltoporin at the single channel level. *FEBS Lett.* 476:224–228.

Bezrukov, S. M., and I. Vodyanoy. 1993. Probing alamethicin channels with water-soluble polymers. *Biophys. J.* 64:16–25.

Bezrukov, S. M., I. Vodyanoy, R. A. Brutyan, and J. J. Kasianowicz. 1996. Dynamics and free energy of polymers partitioning into a nanoscale pore. *Macromolecules.* 29:8517–8522.

Bezrukov, S. M., I. Vodyanoy, and V. A. Parsegian. 1994. Counting polymers moving through a single ion channel. *Nature.* 370:279–281.

Blachly-Dyson, E., S. Z. Peng, M. Colombini, and M. Forte. 1990. Alteration of the selectivity of the VDAC ion channel by site-directed mutagenesis: implication for the structure of a membrane ion channel. *Science (Wash. DC).* 247:1233–1236.

Bustamante, J. O., J. A. Hanover, and A. Liepins. 1995. The ion channel behavior of the nuclear pore complex. *J. Membr. Biol.* 146:239–251.

Chen, Y. D. 1975. Fluctuations and noise in kinetic systems. III. Cycling steady-state models. *J. Theor. Biol.* 55:229–243.

Colombini, M. 1994. Anion channels in the mitochondrial outer membrane. *In* Current Topics in Membranes, Vol. 42. W. Guggino, editor. Academic press, San Diego, CA. 73–101.

Colombini, M., E. Blachly-Dyson, and M. Forte. 1996. VDAC, a channel in the outer mitochondrial membrane. *In* Ion Channels, Vol. 4. T. Narahashi, editor. Plenum Press, New York. 169–202.

Conti, F., and E. Wanke. 1975. Channel noise in nerve membranes and lipid bilayers. *Quart. Rev. Biophys.* 8:451–506.

DeFelice, L. J. 1981. Introduction to Membrane Noise. Plenum Press, New York.

Dische, M. 1953. Qualitative and quantitative colometric determination of heptoses. *J. Biol. Chem.* 204:983–997.

Flörke, H., F. P. Thinnes, H. H. Winkelbach, U. Stadtmüller, G. Paetzold, C. Morys-Wortmann, D. Hesse, H. Sternbach, B. Zimmermann, P. Kaufmann-Kolle, M. Heiden, A. Karabinos, S. Reymann, V. E. Lalk, and N. Hilschmann. 1994. Channel active mammalian porin, purified from crude membrane fractions of human B lymphocytes and bovine skeletal muscle, reversible binds adenosine triphosphate (ATP). *Biol. Chem. Hoppe-Seyler.* 375:513–520.

Freitag, H., R. Benz, and W. Neupert. 1983. Isolation and properties of the porin of the outer mitochondrial membrane from *Neurospora crassa*. *Methods Enzymol.* 97:286–294.

Gellerich, F. N., and W. Kunz. 1987. Cause and consequences of dynamic compartmentation of adenine nucleotides in the mitochondrial intermembrane space in respect to exchange of energy rich phosphates between cytosol and mitochondria. *Biomed. Biochim. Acta.* 46:S545—S548.

Gellerich, F. N., Z. A. Khuchua, and A. V. Kuznetsov. 1993. Influence of the mitochondrial outer membrane and the binding of creatine kinase to the mitochondrial inner membrane on the compartmentation of adenine nucleotides in the intermembrane space of rat heart mitochondria. *Biochim. Biophys. Acta.* 1140:327–334.

Heinemann, S. H., and F. J. Sigworth. 1990. Open channel noise. V. Fluctuating barriers to ion entry in gramicidin A channels. *Biophys. J.* 57:499–514.

Henrickson, S. E., M. Misakian, B. Roberston, and J. J. Kasianowicz. 2000. Driven DNA transport into an asymmetric nanometer-scale pore. *Phys. Rev. Lett.* 85:3057–3060.

Hilty, C., and M. Winterhalter. 2001. Facilitated substrate transport through membrane proteins. *Phys. Rev. Lett.* 86:5624–5627.

Hodge, T., and M. Colombini. 1997. Regulation of metabolite flux through voltage-gating of VDAC channels. *J. Membr. Biol.* 157:271–279.

Kasianowicz, J. J., and S. M. Bezrukov. 1995. Protonation dynamics of the alpha-toxin channel from spectral analysis of pH dependent current fluctuations. *Biophys. J.* 69:94–105.

Kasianowicz, J. J., E. Brandin, D. Branton, and D. Deamer. 1996. Characterization of individual polynucleotide molecules using a membrane channel. *Proc. Natl. Acad. Sci. U.S.A.* 93:13770–13773.

Krasilnikov, O. V., R. Z. Sabirov, V. I. Ternovsky, P. G. Merzliak, and J. N. Muratkhodjaev. 1992. A simple method for the determination of the pore radius of ion channels in planar lipid bilayer membranes. *FEMS Microbiol. Immunol.* 105:93–100.

Machlup, S. 1954. Noise in semiconductors: spectrum of a two-parameter random signal. *J. Appl. Physics.* 25:341–343.

Mannella, C. 1982. Structure of the outer mitochondrial membrane: ordered arrays of pore-like subunits in outer-membrane fractions from *Neurospora crassa* mitochondria. *J. Cell Biol.* 94:680–687.

Mannella, C. A., X. W. Guo, and B. Cognon. 1989. Diameter of the mitochondrial outer membrane channel: evidence from electron microscopy of frozen-hydrated membrane crystals. *FEBS Lett.* 253:231–234.

Meller, A., L. Nivon, E. Brandin, J. Golovchenko, and D. Branton. 2000. Rapid nanopore discrimination between single polynucleotide molecules. *Proc. Natl. Acad. Sci. U.S.A.* 97:1079–1084.

Merzlyak, P. G., L. N. Yuldasheva, C. G. Rodrigues, C. M. M. Carneiro, O. V. Krasilnikov, and S. M. Bezrukov. 1999. Polymeric nonelectrolytes to probe pore geometry: application to the α-toxin transmembrane channel. *Biophys. J.* 77:3023–3033.

Montal, M., and P. Mueller. 1972. Formation of biomolecular membranes from lipid monolayers and a study of their electrical properties. *Proc. Natl. Acad. Sci. U.S.A.* 69:3561–3566.

Neher, E., and C. F. Stevens. 1977. Conductance fluctuations and ionic pores in membranes. *Ann. Rev. Biophys. Bioeng.* 6:345–381.

Nekolla, S., C. Andersen, and R. Benz. 1994. Noise analysis of ion current through the open and the sugar-induced closed state of the LamB channel of *Escherichia coli* outer membrane: evaluation of the sugar binding kinetics to the channel interior. *Biophys. J.* 66:1388–1397.

Nossal, R., and H. Lecar. 1991. Molecular and Cell Biophysics. Addison-Wesley Publishing Company, Redwood City, CA.

Parsegian. V. A., S. M. Bezrukov, and I. Vodyanoy. 1995. Watching small molecules move: interrogating ionic channels using neutral solutes. *Biosci. Rep.* 15:503–514.

Peng, S., E. Blachly-Dyson, M. Forte, and M. Colombini. 1992. Large scale rearrangement of protein domains is associated with voltage gating of the VDAC channel. *Biophys. J.* 62:123–135.

Pietrobon, D., B. Prod'hom, and P. Hess. 1988. Conformational changes associated with ion permeation in L-type calcium channels. *Nature.* 333:373–376.

Prod'hom, B., D. Pietrobon, and P. Hess. 1987. Direct measurement of proton transfer rates to a group controlling the dihydropyridine-sensitive Ca^{2+} channel. *Nature.* 329:243–246.

Rostovtseva, T., and M. Colombini. 1996. ATP flux is controlled by a voltage-gated channel from the mitochondrial outer membrane. *J. Biol. Chem.* 271:28006–28008.

Rostovtseva, T., and M. Colombini. 1997. VDAC channels mediate and gate the flow of ATP: implications for the regulation of mitochondrial functions. *Biophys. J.* 72:1954–1962.

Rostovtseva, T. K., and S. M. Bezrukov. 1998. ATP transport through a single mitochondrial channel, VDAC, studied by current fluctuation analysis. *Biophys. J.* 74:2365–2373.

Rostovtseva, T. K., T.-T. Liu, M. Colombini, V. A. Parsegian, and S. M. Bezrukov. 2000. Positive cooperativity without domains or subunits in a monomeric membrane channel. *Proc. Natl. Acad. Sci. U.S.A.* 97: 7819–7822.

Rostovtseva, T. K., E. M. Nestorovich, and S. M. Bezrukov. 2001. Partitioning of different sized poly-(ethylene glycol)s into OmpF porin. *Biophys. J.* In press.

Sigworth, F. J. 1985. Open channel noise. I. Noise in acetylcholine receptor currents suggests conformational fluctuations. *Biophys. J.* 47:709–720.

Sherman-Gold, R., editor. 1993. The Axon Guide for Electrophysiology and Biophysics Laboratory Techniques. Axon Instruments, Inc. Foster City, CA.

Song, J., C. Midson, E. Blachly-Dyson, M. Forte, and M. Colombini. 1998. The topology of VDAC as probed by biotin modification. *J. Biol. Chem.* 273:24406–24413.

Van Driessche, W. 1994. Noise and impedance analysis. *In* Methods in Membrane and Transporter Research. J. A. Schafer, G. Giebisch, P. Kristensen, and H. H. Ussing, editors. Landes Co., Austin, TX. 27–80.

Vander Heiden, M. G., N. S. Chandel., X. X. Li, P. T. Schumacker, M. Colombini, and C. B. Thompson. 2000. Outer mitochondrial membrane permeability can regulate coupled respiration and cell survival. *Proc. Natl. Acad. Sci. U.S.A.* 97:4666–4671.

Vander Heiden, M. G., X. X. Li, E. Gottlieb, R. B. Hill, C. B. Thompson, and M. Colombini. 2001. Outer mitochondrial membrane permeability can regulate coupled respiration and cell survival. *J. Biol. Chem.* 276: 19414–19419.

Weast. R. C.1979. Handbook of Chemistry and Physics. CRC Press, Inc. Boca Raton, FL.